

Butadiene rubbers: topological constraints and microscopic deformation by mechanical and small angle neutron scattering investigation

Heike Menge (✉), Wim Pyckhout-Hintzen¹, Gerd Meier^{1,2}, Ekkehard Straube

Martin-Luther-University Halle-Wittenberg, Department of Physics, Friedemann-Bach-Platz 6, D-06108 Halle/Saale, Germany

¹ Research Center Jülich, Institute of Solid State Research (IFF), D-52425 Jülich, Germany

² Max-Planck-Institute of Polymer Research, PF 3148, D-55021 Mainz, Germany

e-mail: menge@physik.uni-halle.de, Tel.: + 49 (0)345 55 25 595, Fax: +49 (0)345 55 27 161

Received: 20 November 2001 / Revised version: 5 March 2002 / Accepted: 5 March 2002

Summary

Results of stress-strain measurements are reported for butadiene rubbers of varying crosslink density. The fluctuation of the effective tube diameter of the polymer networks was investigated under uniaxial elongation by mechanical measurements as well as by small angle neutron scattering (SANS) which probe the local orientation on a segmental scale. The effect of topological constraints on the microscopic deformation of the butadiene network chains is well described within a tube approach. For the first time, experiments at large deformations and for polydisperse sample are presented. Excellent agreement between the statistical mechanical model and the experimental results is obtained.

Introduction

The characterization of the complex phenomena appearing in the polymeric systems during their deformation has become a field of intensive investigation in order to get more detailed relationships between molecular orientation and mechanical properties. A better molecular understanding of crosslinked rubbery systems can be obtained by a combined analysis of the mechanical behaviour with a study of chain segmental orientation accompanying macroscopic sample deformation. Whereas the strain dependence of the stress is the most common quantity to assess elasticity theories, experimental determination of segmental orientation is particularly informative for a molecular understanding of the network behaviour. All the Fourier transform (FTIR), the deuterium nuclear magnetic resonance (²H nmr) and the small angle neutron scattering (SANS) techniques directly measure the orientation of specific labels on a chain relative to a laboratory-fixed axis, the orientation being suitable induced by stretching the sample uniaxially. An improved understanding of stress-strain properties and especially the microscopic deformation of elastic chains in ideal polymer networks in the absence of fillers is provided through analysis of the structure factor $S(\mathbf{Q})$ of a single chain under strain, firmly embedded inside a polymer network. SANS is the only available bulk method to be pursued to date. Its wave vectors range,

covering molecular scales down to the segmental basis unit in polymers allows the ultimate investigation of both chain deformation and chain fluctuation on all length scales of interest. Two-dimensional neutron scattering patterns obtained on networks at different strains were recently interpreted in terms of a tube constraint model [1, 2]. This description led to the static determination of the tube confinement parameter which is of dynamic origin and confirmed its nonaffine deformation dependence. Mechanical investigation are in agreement with the power law exponent $\nu = 1/2$ but are too insensitive to discern between an affine behavior ($\nu=1$) and the theoretical predictions of the tube model.

Experimental and theoretical background

The elastomeric networks under study were based on partially CD₂-deuterated poly(butadiene) PB-d₄ of *different* microstructure, molar masses of the precursor chains and mass distribution, resp.. The deuterated polymers were mixed in a ratio 1:9 with a corresponding commercial poly(butadiene) with nearly the same parameters. An amount of 0,5 phr Dicumyl peroxide (DCP) was used as crosslinking agent for the networks under study here. All samples were vulcanised in a vulcameter press at 145 °C and 100 bar for 1h. The network characteristics given in table 1 were investigated by mechanical and swelling measurements as well as from proton and deuteron nmr transverse magnetisation decays [3-7] using a two-component model [6,7].

Table 1: Characteristics of primary polymer chains and resulting networks, M is the molar mass, the indices N,W indicate the number and the weight average, resp., U is polydispersity

Sample	A	C	E	A-05	C-05	E-05
M _N (1,4-PB)	120.000	125.000	61.000	-	-	-
M _W (1,4-PB)	450.000	129.000	64.000	-	-	-
U (1,4-PB)	3,75	1,03	1,05	-	-	-
M _N (1,4-PB-d ₄)	190.000	135.000	50.000	-	-	-
M _W (1,4-PB-d ₄)	700.000	140.000	52.000	-	-	-
U(1,4-PB-d ₄) = M _w /M _n	3,68	1,04	1,04	-	-	-
Microstructure	97% 1,4-cis	cis/trans/vinyl (40 / 50 / 10 %)		-	-	-
Amount DCP (phr)	-	-	-	0,5	0,55	0,64
M _C (mechan.) (g/mol)	-	-	-	7590	3000	5000
M _C (swelling) (g/mol)	-	-	-	4300	2700	5800
M _C (¹ H-NMR) (g/mol)	-	-	-	8000	3040	4700
M _C (² H-NMR) (g/mol)	-	-	-	8200	5100	6270
β ~ 0,26 ln(M _C /M _w -1)	-	-	-	~ 1	0,92- 0,94	0,56- 0,62

The uniaxial *stress-strain* data at room temperature were analyzed using the earlier mentioned tube approach developed by Heinrich et al. [8, 9, 10]. In this model, the

reduced stress σ_M (Mooney stress) is expressed as (macroscopic deformation ratio λ)

$$\sigma_M = \frac{\sigma}{\lambda - \lambda^{-2}} = G_C + G_n f(\lambda) \quad (1)$$

with

$$f(\lambda) = \frac{2(\lambda^{\beta/2} - \lambda^{-\beta})}{\beta(\lambda^2 - \lambda^{-1})} \quad (2)$$

G_C represents the crosslink distribution and G_n the constraint contribution to the modul which are both connected with molecular parameters [10]. Their approach predicts for a deformed network with the main axis deformation ratios λ_μ a pronounced nonaffine deformation of the equilibrium tube diameter d_0 given as

$$d_\mu = d_0 \lambda_\mu^{v\beta} \quad (3)$$

with $v = 1/2$. The relaxation of the deformed tube from the deformed state to an undeformed tube in equilibrium is described by β . For highly crosslinked dry networks made from long primary chains, β takes values near 1,0 [10]. Values of $\beta \ll 1$ indicate a low number of crosslinks per primary chain and consequently a large number of network defects, which favor constraint release processes. The contribution of chemical crosslinks G_C to the modulus is given for a tetra-functional network

$$G_C = A \left(\frac{d_c}{R_c} \right) RT (v_c - v_n) \quad (4)$$

where v_c and v_e are the network crosslink density and the density of elastically active crosslinks, resp., $A(d_c/R_c)$ is a microstructure factor which depends on the ratio between the fluctuation range d_c of the crosslinks first introduced by Kästner [11] and the end-to-end-distance R_c of a network chain. In the tube approach, d_c is set equal to the fluctuation range of the segment d_0 , which in turn depends on the length of the statistical segment. The microstructure factor is defined as:

$$A = 1 - \frac{2}{f} \left[1 - \frac{2K \exp(-K^2)}{\sqrt{\pi} \operatorname{erf}(K)} \right] \quad (5)$$

with $K = (3f/2)^{1/2} (d_c/R_c)$ and f as the functionality of the crosslinks. According to Heinrich et al. [10], equ. (5) takes into account the fact that the constraints acting on a crosslink are stronger than the constraints acting on segments of network chain distant from crosslink. . Note that this approach reduces to the Mooney-Rivlin form ($f(\lambda) = 1/\lambda$) for $\beta = v = 1$.

SANS data were recorded using the KWS1 and KWS2 spectrometers at the FRJ-2 reactor in the research center Jülich (IFF) with a neutron wavelength of $\lambda_N = 0,7$ nm and a wave length spread $\lambda_N/\Delta\lambda_N$ of about 18% and 9%, resp.. The detector distances were varied with 2 m, 8 m and 20 m, providing an experimental range of 0,008 to 0,14 \AA^{-1} (corresponding to a detector distance of 2 - 8 m, which is mostly shown in the

figures), in term of the scattering vector $Q = (4\pi/\lambda_N)\sin(\theta/2)$ with θ the scattering angle. The incoherent background was separately measured from the fully unlabeled network of comparable crosslink density and subtracted.

The microscopic matrix chain deformation in the network is evaluated using the tube model of rubber elasticity [10] which successfully describes the chain deformations of polyisoprene networks [2, 12] This model includes the topological constraints due to the other matrix chains in terms of an harmonic potential modeling thereby the range of localization in the tube picture. Recently, the strength of this model to predict properties was tested against more complicated than the uniaxial deformations used in most experiments [13] The scattering function for a single labeled path in such a matrix-network, $S(\mathbf{Q})$, is

$$S(Q) = 2 \int_0^1 d\eta \int_0^\eta d\eta' \prod_{\mu} \exp \left\{ \begin{array}{l} - (Z_{\mu} \lambda_{\mu})^2 (\eta - \eta') - Z_{\mu}^2 (1 - \lambda_{\mu}^2) \frac{d_{\mu}^2}{2\sqrt{6}R_g^2} \\ \left[1 - \exp \left(- \frac{\eta - \eta'}{d_{\mu}^2 / 2\sqrt{6}R_g^2} \right) \right] \end{array} \right\} \quad (6)$$

where R_g is the radius of gyration of the labeled path in the undeformed isotropic state and $Z_{\mu} = Q_{\mu}R_g$ is a component of the reduced scattering wave vector \mathbf{Q} in the main axis system of the deformation tensor acting on the chain level with the components λ_{μ} ($\mu = x, y, z$). $d_{\mu}^2 = \lambda_{\mu}^{2\nu} d_0^2$ ($\nu = 1/2$ for nonaffine deformation) is the square of the tube diameter in principal direction with the deformation ratio λ_{μ} . Introducing $\lambda_{\mu}^2 \rightarrow \lambda_{\phi}^2 = \lambda^2 \cos^2\phi + (1/\lambda) \sin^2\phi$ where now any direction ϕ with the strain axis is observed, allows the description of all off-axis intensities in the 2d-plane. Thereby taking profit of all information instead of relying on the axis data. The procedure involves the calculation of equ. (6) in 4000 channels and needs a splining algorithm. η and η' are dimensionless contour length coordinates extending over the labeled paths of the chains. The calculation of equ. (6) with $\lambda_{\mu} = \lambda_{\mu} = 1$ yields the isotropic result (Debye curve). The macroscopic stretching ratio λ ($=l/l_0$) was determined from the distance between two marks before and after stretching within an accuracy of 5%. The data were absolutely calibrated by means of the known incoherent level of polyethylene.

Results and discussion

For the evaluation of the network parameters from the stress-strain data sets (experimental testing speed was set to 0.4 mm/min on stripes of 50 mm x 5 mm x 1mm), the constraint part of the G-modulus G_n and the crosslink part G_C were determined by a linear least-square fit of the Mooney stress σ_M versus $f(\lambda)$ (modified Mooney-plot) starting with $\beta = 1$. With G_n and G_C , the parameter β was recalculated. The estimated values for the sample A-05 (high-cis) under study are $G_n = 0,37$ MPa and $G_C = 0,23$ MPa. From the values of G_n and G_C , information on the parameters of the network structure can be extracted. For the estimation of the parameters associated with the constraint it is necessary to know the value of the Kuhn statistical segment length, l_{st} , and the mass of a Kuhn statistical segment M_{st} for the butadiene rubber. Both values were taken from literature being $l_{st} = 0,757$ nm and $M_{st} = 70$ g/mol for the

high cis butadiene rubber and $l_{st} = 0,808$ nm and $M_{st} = 74$ g/mol for the atactic butadiene rubber, respectively [14, 15]. In case of the high cis rubber, the ratio of the tube diameter d_0 and the mean radius of gyration $\langle Rg \rangle$ of a network chain was calculated as 0,208 from stress-strain curve by equ. (5). The fitted tube diameter prefactor α is 5,6 for the high cis content. From these data, a tube diameter d_0 of 2,3 nm (23 Å) is estimated using equ. (7)

$$d_0 = 0.57 (\alpha \beta)^{1/2} \left(\frac{k T l_{st}}{G_n} \right)^{1/4} \quad (7)$$

with k is the Boltzmann constant and T is the temperature. The accuracy of the given tube diameter is within $\pm (3 - 4)$ Å.

For the atactic networks, the ratio of the tube diameter d_0 and the mean radius of gyration $\langle Rg \rangle$ was estimated from the fit of the stress-strain curve (equ. (5)) to 0.33 and 0.248 for C and E, respectively. The tube diameter prefactor α estimated as 8.5 from melts was used. The tube diameters for C-05 and E-05 are estimated (from equ. (7)) to $d_0 = 40$ Å and $d_0 = 27$ Å, resp., with $\beta = 1,0$. The opposite trend of the tube diameter with the crosslink density for both atactic networks results from the very limited experimental strain range, which was not really sufficient for an accurate determination of the tube diameter. The mean molecular mass of a network chain M_c (between two adjacent crosslinks) for the polymer networks under study estimated from stress-strain, from swelling and from nmr relaxation (1H , 2H) measurements are in close agreement [3-5]. Details are given in table 1 and in the references [3-5].

The SANS data of butadiene networks obtained in the strained state, are interpreted in terms of the tube model for polymer networks as mentioned above. Here, we present 2D SANS data on labeled chains crosslinked within a network for different degrees of strain. Depending on strain, the 2D patterns of the butadiene networks under study exhibit a significant transition from the expected ellipsoidal to a lozengic shape as already discussed and observed for poly(isoprene) networks under uniaxial stress [2]. On the basis of the mean-field tube model, Straube et al. [1, 2] showed that the 2D scattering function as a function of strain (equ. (6)) provides an explanation of this new anisotropy. A good fit of the 2D scattering data could be obtained using the power-law exponent $\nu = 1/2$ as predicted for a nonaffine deformation behaviour at constant tube diameter. Care must be taken in the derivation of molecular parameters from this model due to the non-negligible polydispersity U of the labeled chain A-05.

An analysis from the isotropic SANS spectrum via the Guinier or Zimm approximation yields a first approximation of the Gyration radii which is of the z-type. It is clear that this is inferior to characterize the topology of the network. In anisotropic spectra the parameter d_0/R_g only contributes approximately 5%. The agreement is found to be satisfactory with the estimates of chain dimension relations of monodisperse material $Rg_z = (0,3-0,35)\sqrt{M_w}$. In the polydisperse case, assuming the relationships

$$\frac{Rg_z^2}{Rg_w^2} = \frac{1 + 2x}{1 + x} \quad (8)$$

with $x = U - 1$, a correction from about 1,30 is found for Rg_w to Rg_z in. The estimated value for the networks are 152, 119 and 73 Å respectively for network A, C and E.

We found: $R_g=119 \text{ \AA}$ (Guinier)/ 135 \AA (Zimm) for network C-05, $R_g=81 \text{ \AA}$ (Guinier)/ 100 \AA (Zimm) for network E-05 and $R_g=167 \text{ \AA}$ for network A-05.

In the literature, results are given for similar polybutadiene networks by Straube et al. from Kratky representations [1] with $d_0 \sim 41 \text{ \AA}$. The authors argued there that the agreement could be increased if two-dimensional fits are available which are used now in this study. For the networks C-05 and E-05 prepared from a narrow molar mass distribution a perfect fit of the 2D scattering pattern was obtained with one set of parameters, R_g , d_0 , and the constraint release exponent β . The fits yielded values for β varying between 1 and 0,65 and average tube parameters d_0/R_g between 0,242 and 0,276-0,366, resp. The fluctuation range therefore is $d_0 \sim 33 \text{ \AA}$ and 26 \AA for $\beta=1$. These values are in good agreement with the previous given results [1, 16]. However, the resulting fit of the 2D scattering pattern for network E-05 could be even improved allowing the parameter β to be in the order of 0,6 which is in excellent agreement with an empirical expression found by Westermann [17] for several polyisoprene networks varying in M_C and M_w :

$$\beta \cong 0,26 \ln nc \quad (9)$$

with $nc = (M_w/M_C) - 1$ as the number of knots per primary chain. This is at least a strong indication that β and d_0 are related and coupled. Based on the polymer data given in Table 1 the constraint release exponent β could be approximated to be about 0,92 - 0,94 for network C-05 and 0,56 - 0,62 for network E-05 at constant tube diameter. This is justified in terms of the mean field tube model and the existing rubbery plateau in uncrosslinked melts. The restricted fluctuation of the crosslinks is a secondary effect, not to be different from the segmental fluctuations as found from NSE measurements on PDMS junctions [18]. The low β value for the network E-05 is consistent with recently published nmr relaxation results [3, 4]. In this nmr study a large number of network defects (22 % of segments in pendant chains) compared to 8 % in the C-05 network has been observed.

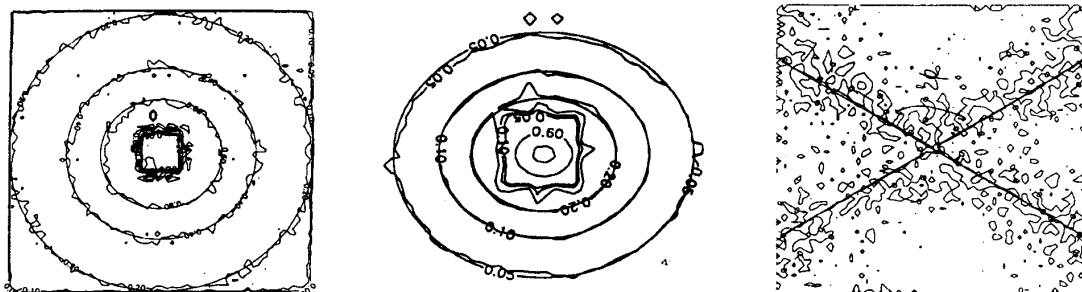


Fig. 1. Experimental SANS pattern from deformed BR-network E-05 and best-fit curves for different strains $\lambda = 1,0$ and $1,15$. The stretching direction is vertical. The fit parameters were obtained as follows (see table 2): $d_0 = 35 \text{ \AA}$ at $R_g=96 \text{ \AA}$ and $\lambda = 1,15$ with $\beta=0,6$ indicating a large number of network defects which are isotropically relaxed but still scatter. The microscopic strain determined from an isotropic angle line plot to be $\lambda = 1,12$ [2] is in excellent agreement with the applied macroscopic extension ration of the sample. This angle is determined from the intersection of deformed and undeformed spectrum, where the condition $\lambda\phi=1$ is met. Measurements of ϕ yields immediately the microscopic strain λ^β on the chain level. Left: low Q-range (8m), middle: high Q-range (2m), right: isointensity plot.

Table 2: Fitting results from 2D SANS scattering pattern within the tube approach ($\nu = 1/2$)

Sample	λ	d_0 (Å)	R_g (Å)	β	d_0/R_g
C-05	1,0	-	139	-	-
	1,2	34	140	1,0	0,243
E-05	1,0	-	95	-	-
	1,15	26	94	1,0	0,277
	1,15	35	96	0,6	0,365
A-05	1,0	-	156	-	-
	2,6	35	156	1,0	0,224
	4,2	35	156	1,0	0,224

For the network A-05 (based on a broad molar mass distribution of the precursor polymer chains) a relatively good fit with a unique data set could be achieved, too with $d_0 = 35$ Å and $R_g = 156$ Å. However, there are some deviations mainly due to the broad primary chain length distribution (table 1) which is not included explicitly in the scattering function (equ. (6) is only valid for monodisperse primary chains). This is probably due to the limited scattering vector range. The radius of gyration corresponding to a peak molecular weight taken as $M_p \approx \sqrt{M_w M_z}$ is about 325 Å in the isotropic state. If this chain is stretched to the deformation $\lambda = 2.6$ or 4, the parallel component completely disappears into the beam stop of the detector, prohibiting in this way a unique determination. Only the perpendicular component remains. At the same time, due to the d_0/R_g dependence in equ. (6) also the constraint contribution is small and a fairly monodisperse ensemble seems to work well in the first approximation. The contribution therefore to d_0/R_g is small and a fairly monodisperse ensemble seems to work well in the first approximation. The fits in fig. 2 show considerable agreement with the model along both principal axes. At the highest strain the shape of the lozenge is too pronounced, however. Since the agreement is good at $\lambda = 2.6$, we might speculate that another process which tends to smear the tube constraints like mechanical rupture which relaxes the points of stress in the rubber, sets in. Crystallization is ruled out for the same reason that the spectrum is less anisotropic than predicted. Equally well would be the explanation by resolution effects in the 2d-plane. Since these are not straight forward for 2d-intensities they were neglected.

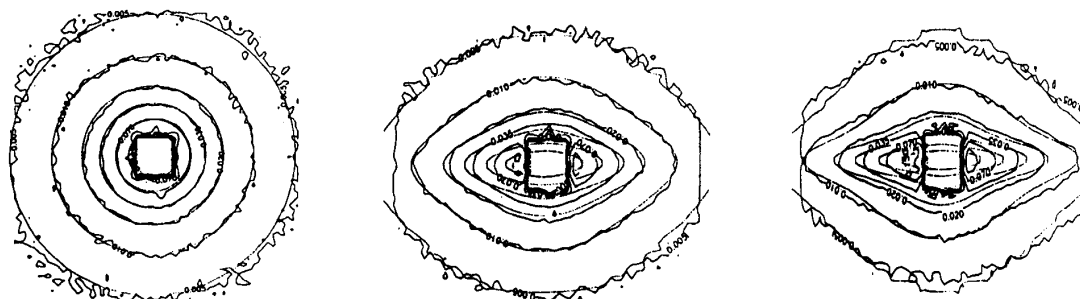


Fig. 2. Experimental SANS pattern from deformed high-cis-BR-network A-05 and best-fit curves for different strains $\lambda = 1.0, 2.6$ and 4.2 . The stretching direction is vertical. The fit parameters are given in table 2. The Q-range shown here corresponds to a detector distance of 8 m ($Q = 0,008 \text{ \AA}^{-1}$).

At this point a comparison with the tube confinement parameters from mechanical analysis is to be made. Tube parameters for atactic polybutadiene networks given in previous papers [1] are in also the range between 25 and 35 Å. Another source of data obtained on high cis-polybutadiene radiation-crosslinked networks with long primary chains ($M_w \approx 3,0 \times 10^5$ g/mol) [19] yielded $d_0 \sim 32 - 34$ Å in a range of network chains M_C assuming $\beta = 1$, however. Smaller tubes are already obtained in the case of higher crosslink densities [20].

Consequently, we confirm previous results on polyisoprene [2, 12] and polybutadiene networks [1, 16, 19]. The tube model for entangled polymer systems with predominant constraint contributions and their proposed simple nonaffine deformation dependence gives a good description of the statistical mechanics of rubberelastic networks even at large deformation ratios and for polydisperse network systems. The data proof that for less-crosslinked rubbers the unique determination of β or tube parameter is hampered and extra information must be put into the interpretation.

Acknowledgements. The authors kindly acknowledge Dr. Stephan Westermann for fruitful discussions. H.M. wishes to thank Ms. S. Hotopf and Ms. M. Hintzen for sample preparation and polymer characterization, and additionally the Max-Planck-Institute of polymer research in Mainz and the DFG (project Schn 407/2-1, -2; Sonderforschungsbereich (SFB) no. 418) for financial support. The financial support of the BMBF project 03EW4MP1 is gratefully acknowledged.

References

- 1 Straube, E.; Urban, E.; Pyckhout-Hintzen, W.; Richter, D. (1994) *Macromolecules* 27: 7681
- 2 Straube, E.; Urban, E.; Pyckhout-Hintzen, W.; Richter, D.; Glinka C. J. (1995) *Phys. Rev. Lett.* 74: 4464
- 3 Menge, H.; Hotopf, S.; Heuert, U.; Schneider, H. (2000) *Polymer* 41: 3019
- 4 Menge, H.; Hotopf, S.; Schneider, H. (2000) *Polymer* 41: 4189
- 5 Menge, H.; Ekanayake, P.; Ries, M. E.; Brereton, M. G.; Findeisen, M. (1999) *Polym. Bull.* 43: 371
- 6 Simon, G.; Schneider, H. (1991) *Makromol. Chem., Macromol. Symp.* 52: 233
- 7 Simon, G.; Gronski, W.; Baumann, K. (1992) *Macromolecules* 25: 3624 and references therein
- 8 Heinrich, G.; Straube, E. (1983) *Acta Polym.* 34: 589
- 9 Heinrich, G.; Straube, E. (1987) *Polym. Bull.* 17: 247
- 10 Heinrich, G.; Straube, E.; Helmig G. (1988) *Adv. Polym. Sci.* 85: 33
- 11 Kästner, S. (1981) *Colloid Polym. Sci.* 259: 499
- 12 Westermann, S.; Urban, V.; Pyckhout-Hintzen, W.; Richter, D.; Straube, E. (1996) *Macromolecules* 29: 6165
- 13 Kaliske, M.; Heinrich, G. (1997) *Comput. Theor. Polym. Sci.* 7: 227
- 14 Aharoni, S. M. (1983) *Macromolecules* 16: 1722
- 15 Aharoni, S. M. (1986) *Macromolecules* 19:426
- 16 Pyckhout-Hintzen, W.; Springer, T.; Forster, F.; Gronski, W.; Frischkorn, C. (1991) *Macromolecules* 24: 269
- 17 Westermann, S. (1998) PhD Thesis, Univ. Münster (Westfalen), Germany
- 18 B. Ewen, D. Richter (1988) "Molecular basis of polymer networks" in "Polymer motion in dense systems" Springer Proc. Phys. 42: 1288
- 19 Pyckhout-Hintzen, W.; Müller, B.; Springer, T. (1993) *Makromol. Chem., Macromol. Symp.* 76: 121
- 20 Matzen, D.; Straube, E. (1992) *Colloid Polym. Sci.* 270: 1